

MODELING METHODS FOR HIGH-FIDELITY ROTORCRAFT FLIGHT MECHANICS SIMULATION

M. Hossein Mansur and Mark B. Tischler
U.S. Army AVSCOM, Aeroflightdynamics Directorate
Ames Research Center, Moffett Field, CA 94035-1000 U.S.A.

Menahem Chaimovich, Aviv Rosen, and Omri Rand
Dept. of Aerospace Engineering
Technion-Israel Institute of Technology
Haifa 32000, Israel

Abstract

This paper is a first report on the cooperative effort in helicopter Flight Mechanics Modeling being carried out under the agreements of the United States-Israel Memorandum of Understanding. It presents two different models for the AH-64 Apache Helicopter which mainly differ in their approach to modeling the main rotor. The first model, referred to as "BEMAP" (Blade-Element Model for the APache), was developed at the Aeroflightdynamics Directorate, Ames Research Center, and is the only model of the Apache to employ a direct blade-element approach in calculating the coupled flap-lag motion of the blades and the rotor force and moment. The second model was developed at the Technion-Israel Institute of Technology and uses a harmonic approach to analyze the rotor. This approach allows different levels of approximation, ranging from "first-harmonic" (similar to a tip-path-plane model) to "complete high-harmonics" (comparable to a blade-element approach). The development of the two models is outlined and the two are compared using available flight test data.

Introduction

Mathematical models intended for flight mechanics applications are well thought out compromises between simplicity and accuracy. Generally speaking, the more sophisticated a model is, the more accurately it can match the responses of the actual flight vehicle. Sophistication, however, brings with it increased costs both in development and in eventual use. For example, models such as CAMRAD (Ref 1) are highly sophisticated and multidisciplinary but are cumbersome to use for parametric studies in handling qualities and are unsuitable for real-time applications. Lack of sophistication, on the other hand, can lead to unacceptable inaccuracies. For example, stability-derivative-type models, such as TMAN (Ref 2), while very simple for real-time applications, can lead to

erroneous conclusions since they are only applicable to a very limited region of the flight envelope, and are not very accurate even there. A careful determination of the level of sophistication needed to achieve the required accuracy is therefore necessary, especially if the model is intended for real-time in addition to nonreal-time use.

The single most important module of any component-type helicopter mathematical model is the main rotor. This is true not only because the rotor is singularly responsible for almost all the forces and moments, but also because all other components are significantly affected by the rotor. The sophistication and accuracy of the rotor module, therefore, largely determines the sophistication and accuracy of the entire model. There are several approaches currently used in flight mechanics for modeling the main-rotor. These include 1) the tip-path-plane approach, 2) the rotor-map approach, and 3) the direct blade-element approach. All of the above approaches are inherently similar in that they all start with a strip-theory modeling of each blade. In the tip-path-plane approach, such as that used in ARMCOP (Ref 3), the equations of motion are transformed to a non-rotating frame using the multiblade-coordinate transformation and solved analytically. As a consequence, only very simple linear aerodynamics are considered and effects such as compressibility, blade stall, and reverse flow are neglected.

The rotor-map approach, such as used in FLYRT (Ref 4), was initially developed in order to allow real-time operation of a blade-element rotor. In this approach, a nonreal-time blade-element model is run off-line for a great number of flight conditions and the results recorded in quasi-static look-up tables. The tables are then used by the real-time rotor module to instantly determine the quasi-static rotor forces, moments, and attitudes based on the input parameters. Rotor dynamics are then added to the quasi-static results to complete the rotor output. This approach is also restrictive with regard to modeling secondary effects such as compressibility, stall, and reverse flow.

Finally, in the direct blade-element approach, such as in GEN HEL (Ref 5), the intermediate step of generating output tables is eliminated thanks to the power and speed of the current computers. This allows easy access to the calculations at the elemental level which in turn makes it easier to employ sophisticated aerodynamic theories and account for the secondary effects in detail.

Researchers from the U.S. Army Aeroflightdynamics Directorate and the Technion-Israel Institute of Technology have been working cooperatively under the agreements of the United States-Israel Memorandum of Understanding (MOU) on "Helicopter Flight Control and Display Technology" to evaluate alternative methods of formulating rotor system models for rotorcraft flight-mechanics simulation.

While both research groups have used a strip-theory approach, the implementations are quite different and each has distinct advantages and limitations. The U.S. Army has developed a model based on symbolically generated exact equations of motion and numerical summation of the blade-element forces and moments in a rotating frame. The "Technion Model" uses aerodynamic harmonic functions as forcing terms to the equations of motion expressed in a non-rotating frame. The two models have been configured to represent the AH-64 Apache helicopter (Fig 1), and an enhanced simulation capability for the AH-64 has become available as a result of this work. This paper presents an overview of both modeling approaches and a comparison of the simulated responses against available flight-test data. This comparison of methodology based on a common aerodynamic and flight-test data-base permits a good opportunity to assess the tradeoffs between simplicity and accuracy.

Modeling Methods

This section describes the two methods used for modeling the rotor. The airframe modules for both BEMAP and the Technion Model are essentially the same since they both use look-up tables based on the same set of wind-tunnel data.

Overview of the Approach Used by the U.S. Army

The structure of the Sikorsky GEN HEL main-rotor module (Ref 5) was chosen as the starting point for the new AH-64 main-rotor. This choice was made because the GEN HEL main-rotor was the only readily available blade-element type module usable for real-time operation (Ref 6). The equations for the coupled flap-lag dynamics of each blade were derived symbolically with the aid of the symbolic manipulation program MACSYMA (Ref 7). A Newtonian approach was used for the derivation and no simplifying assumptions were made other than the use of rigid blades. The equations were completely expanded to

allow a close look at the effects of various terms, and to allow relative magnitude analysis on the terms that are often ignored to ensure that they are indeed negligible for the flight condition being considered. The complete equations were retained for this work.

The UH-60 specific equations in the GEN HEL main-rotor module were replaced with the newly derived equations and the UH-60 specific data in the module replaced with the corresponding AH-64 data. The MDHC model of the Apache, known as FLYRT (Ref 4) and obtained under contract to the U.S. Army, was then restructured to allow the upgrading of the model by replacing the main-rotor module. A few other modules also had to be upgraded to support the new blade-element rotor. Finally, the input/output structure of the rotor module was revamped to allow interface with FLYRT instead of GEN HEL. The U.S. model of the AH-64 being used here is therefore a restructured and updated FLYRT employing a blade-element type rotor instead of the model's original map-type main-rotor module. The original FLYRT with the Rotor-Map main-rotor module was recently validated by comparison with available flight data (Ref 8). The same flight data will be used in the present report for ease of comparison.

Formulation of Rotor Equations: As mentioned previously, the equations for the coupled flap-lag motion and the rotor force and moment were derived with the aid of the symbolic manipulation program MACSYMA. Figure 2 depicts the coordinate systems used for the Newtonian derivation. Note that a flap-lag-pitch hinge sequence has been used which does not include the pitch-lag coupling that exists with the flap-pitch-lag hinge sequence of the Apache. It was decided that the improvement in model accuracy afforded by the inclusion of the pitch-lag coupling does not justify the significant increase in equation complexity that results from the inclusion.

First, the hub inertial translational and rotational velocity and acceleration vectors were derived (rotating-shaft frame) based on the rotational and translational velocity and acceleration vectors at the aircraft C.G., and the relative location of the C.G. and the rotor hub. Then, the velocity and acceleration vectors at a given blade-element were derived (rotating-shaft frame), as the sum of the hub motion and the local flapping and lead-lag.

The coupled flap-lag equations of motion were then derived as a balance of inertial, aerodynamic, gravitational, and restraint (flap and lead-lag spring and damping terms) moments about the lead-lag and the flapping hinges. The inertial terms of these equations were compared with a previous, Lagrangian derivation by Chen (Ref 9) and shown to be a perfect match. The rotor force and moment vectors were also derived and MACSYMA was used to generate FORTRAN code corresponding to the new equations. The aerodynamic forces for each blade-element are calculated using swept wing approximations (Ref 5), with

table look-up of lift and drag coefficients as a function of the local angle of attack and Mach number. The look-up tables were constructed based on data available in the "Air Vehicle Technical Description Data for the AH-64A Advanced Attack Helicopter" (Ref 10). Since a good model of the lead-lag dampers was not available, flapping and lead-lag spring and damping terms were included in the equations as a temporary alternative. The values of these parameters were provided by McDonnell Douglas Helicopter Company.

The rotor force and moment vectors were calculated by numerically summing the elemental forces and moments, first over each blade and then over all the blades. Special attention was given to the transfer of moments through each hinge as components along the two axes not aligned with the axis of the hinge. These moments are often ignored by assuming that hinges do not transfer any moments, which, of course, is only true of the components of moments aligned with the axes of the hinges. This may be seen if we look at the detailed derivation of the rotor moments from a blade-element down to the hub. Let ΔF_T , ΔF_R , and ΔF_P be the tangential, radial, and perpendicular components of the forces on a typical blade-element (Fig 2). Then, the elemental force in frame 1 may be written as

$$\begin{aligned} \Delta \bar{F}_{f1} &= \begin{bmatrix} \cos \delta & \sin \delta & 0 \\ -\sin \delta & \cos \delta & 0 \\ 0 & 0 & 1 \end{bmatrix} \begin{Bmatrix} -\Delta F_T \\ \Delta F_R \\ -\Delta F_P \end{Bmatrix} \\ &= \begin{Bmatrix} -\Delta F_T \cos \delta + \Delta F_R \sin \delta \\ \Delta F_T \sin \delta + \Delta F_R \cos \delta \\ -\Delta F_P \end{Bmatrix} \quad (1) \end{aligned}$$

The moment arm from the outer hinge (lead-lag in our case) to the blade-element may be written, in frame 1, as

$$\bar{r}_{\text{moment arm}} = \begin{Bmatrix} r_\delta \sin \delta \\ r_\delta \cos \delta \\ 0 \end{Bmatrix} \quad (2)$$

Therefore, the elemental moment at the outer hinge (lead-lag), which is the cross product of the moment arm and the elemental force, is

$$\Delta \bar{M}_{lag, f1} = \begin{Bmatrix} -r_\delta \Delta F_P \cos \delta \\ r_\delta \Delta F_P \sin \delta \\ r_\delta \Delta F_T \end{Bmatrix} \quad (3)$$

The elemental moment at the inner hinge (flapping) is the sum of the moment transferred through the outer hinge (lead-lag) and the moment due to the shear force at the outer hinge. Therefore, the elemental moment at the inner hinge, in frame 2, may be written as

$$\begin{aligned} \Delta \bar{M}_{flap, f2} &= \begin{Bmatrix} -r_\delta \Delta F_P \cos \delta \\ r_\delta \Delta F_P \sin \delta \\ 0 \end{Bmatrix} \\ &+ \begin{Bmatrix} -\Delta e \Delta F_P \\ 0 \\ [\Delta e \Delta F_T \cos \delta \\ -\Delta e \Delta F_R \sin \delta] \end{Bmatrix} \quad (4) \end{aligned}$$

Finally, the elemental hub moment, in the rotating-shaft frame, may be written as the sum of the moment transferred through the inner hinge and the moment due to shear force at the inner hinge. Therefore, the elemental moment at the hub, in the rotating-shaft frame, may be written as

$$\begin{aligned} \Delta \bar{M}_{hub, rs} &= \begin{Bmatrix} 0 \\ [\tau_\delta \Delta F_P \sin \delta \cos \beta + (\Delta e \Delta F_T \cos \delta \\ -\Delta e \Delta F_R \sin \delta) \sin \beta] \\ [-\tau_\delta \Delta F_P \sin \delta \sin \beta + (\Delta e \Delta F_T \cos \delta \\ -\Delta e \Delta F_R \sin \delta) \cos \beta] \end{Bmatrix} \\ &+ \begin{Bmatrix} [(-\Delta F_T \sin \delta \sin \beta \\ -\Delta F_R \cos \delta \sin \beta \\ -\Delta F_P \cos \beta) e_\beta] \\ 0 \\ (\Delta F_T \cos \delta - \Delta F_R \sin \delta) e_\beta \end{Bmatrix} \quad (5) \end{aligned}$$

Only the second vector of the right-hand side, which represents the moment of the shear force at the inner hinge multiplied by the inner hinge offset, is usually considered in derivations (Ref 5). However, experimentation with introducing the appropriate extra terms in GEN HEL (for the UH-60 lag-flap-pitch sequence) (report by M. H. Mansur to be published as an Army-NASA Technical Memorandum) has shown that the extra terms may also be significant. They were therefore retained for this work.

Overview of Approach Used at the Technion

Researchers of the Faculty of Aerospace Engineering at the Technion have been developing rotorcraft flight mechanics simulation models for the last 10 years (Refs 11-15). The initial approach to rotor modeling was based on a Tip-Path Plane approach, or more accurately, taking into account only the constant and first harmonic of the forcing terms in the rotor equations of motion and the response variables. Recently, the model has been extended and is capable of taking into account higher harmonics also. More details appear in the subsection on the formulation of the rotor equations.

While the rotor represents the most important element of the helicopter, a balanced model requires an appropriate (accurate enough) description of the contribution of other elements of the vehicle. The method of dealing with the contributions of these elements in trim calculations was first described in Ref 14. This method was later extended to include maneuvers and stability calculations as well. A very brief description of the method of calculating these contributions, which include fuselage, tail-rotor, etc., will be presented for the sake of completeness.

1. Fuselage: Inertia contributions are dealt with in an accurate manner and look-up tables, based on wind tunnel tests, are used to calculate the aerodynamic contributions.

2. Tail Rotor: The dynamics include only flapping and the calculations are similar to the main rotor. First-order interference effects between the vertical fin and the tail rotor are included.
3. Vertical fin, wings, stabilizer: The calculations of the contributions of the aerodynamic surfaces are based on look-up tables. Corrections for side-slip and aspect ratio are included.
4. External stores (may include rockets, missiles, fuel tanks, etc.): The inertia contributions are added to the fuselage. Look-up tables are used for the aerodynamic calculations.

Formulation of Rotor Equations: The Technion rotor model is an extension of the model that was described in Refs 11-13. Only a brief description is presented here. More details will appear in forthcoming publications.

The blade's equations of motion are derived using Lagrange's equation. The general form of these equations is

$$[A]\{\ddot{\sigma}\} + \Omega[B]\{\dot{\sigma}\} + \Omega^2[C]\{\sigma\} = \{Q_I\} + \{Q_A\} \quad (6)$$

where $\{\sigma\}$ is the vector of unknowns:

$$\{\sigma\}^T = \langle \beta, \theta_R, \theta_e \rangle \quad (7)$$

and β , θ_R , and θ_e define the angle of flapping, elastic pitch at the blade root, and elastic pitch variations along the blade respectively.

$[A]$, $[B]$, and $[C]$ in Eq (6) are square matrices of order 3 that include all the design details of the rotor and the blades. $\{Q_I\}$ is the forcing vector that includes all the effects except aerodynamics. $\{Q_A\}$ is the forcing aerodynamic vector, defined as

$$\{Q_A\}^T = \langle Q_{\beta A}, Q_{\theta R A}, Q_{\theta_e A} \rangle \quad (8)$$

and $Q_{\beta A}$, $Q_{\theta R A}$, and $Q_{\theta_e A}$ are generalized aerodynamic loads. The expressions for these loads are obtained by applying the principle of virtual work. A special ordering scheme is applied to simplify the equations.

At each time step during the simulation the generalized aerodynamic loads are calculated at a finite number of azimuthal locations. Then, by using a Fast Fourier Transform procedure the generalized aerodynamic loads are expressed in the following harmonic form:

$$\begin{aligned} Q_{\beta A} &= M_{\beta 0} + \sum_{j=1}^{N_j} [M_{\beta C_j} \cos(j\psi) \\ &\quad + M_{\beta S_j} \sin(j\psi)] \\ Q_{\theta R A} &= M_{\theta R 0} + \sum_{j=1}^{N_j} [M_{\theta R C_j} \cos(j\psi) \\ &\quad + M_{\theta R S_j} \sin(j\psi)] \\ Q_{\theta_e A} &= M_{\theta_e 0} + \sum_{j=1}^{N_j} [M_{\theta_e C_j} \cos(j\psi) \\ &\quad + M_{\theta_e S_j} \sin(j\psi)] \end{aligned} \quad (9)$$

where ψ is the blade's azimuth angle and N_j is an input to the computer program. As N_j increases the accuracy increases, but, at the same time, the required computer time is increased as well.

After the three coupled equations of motion of a single blade are obtained, a multiblade coordinate transformation is applied. As a result, each of the three variables β , θ_R , and θ_e is replaced by four new unknowns associated with the multiblade coordinates for a four-bladed rotor: $(\)_0$, $(\)_c$, $(\)_e$, and $(\)_{N/2}$. Thus, Eq (6) for each blade is replaced by the following multiblade equation:

$$\begin{aligned} [A_m]\{\ddot{\tau}\} + [B_m]\{\dot{\tau}\} + [C_m]\{\tau\} \\ + [D_m]\{pq\} + [E_m]\{PC\} \\ + [F_m]\{PC\} + \{f_m\} \\ = M_A \end{aligned} \quad (10)$$

where τ is the vector of rotor variables:

$$\{\tau\}^T = \langle \beta_0, \theta_{R0}, \theta_{e0}, \beta_c, \theta_{Rc}, \theta_{ec}, \beta_s, \theta_{RS}, \theta_{eS}, \beta_{N/2}, \theta_{RN/2}, \theta_{eN/2} \rangle \quad (11)$$

and $\{pq\}$ is the vector of angular rates of the hub and $\{PC\}$ is the vector of collective and cyclic pitch inputs to the main rotor.

$\{M_A\}$ in Eq (10) is the vector of aerodynamic loads after transformation to the multiblade coordinates. This vector is a function of the harmonic coefficients of Eq (9). It should be pointed out that the aerodynamic calculations include dynamic-inflow effects (Ref 16) and aerodynamic interference between the rotor and the fuselage (Ref 17).

Figure 3 represents the aerodynamic flapping moment at the blade root in trimmed horizontal flight at an airspeed of 100 knots. Two cases, one for $N_j = 1$ and the other for $N_j = 4$, are compared. In the case of $N_j = 1$, only the first harmonic terms are considered in the blade flapping motion. The figure shows ($N_j = 1$ actual) that even with only the first harmonic terms included in the blade dynamics, the actual flapping moment includes higher harmonic components. The first harmonic approximation to this actual flapping moment is also shown in the figure ($N_j = 1$

approximate). It may be clearly seen that fairly large deviations exist between the first harmonic approximation and the actual flapping moment.

In the case $N_j = 4$, the first four harmonics are included in the blade dynamics. As may be seen, the actual flapping moment again includes high harmonic components, even above the first four harmonics. The presence of harmonics above the first four is indicated by the slight deviation between the actual flapping moment and its first-four harmonics approximation ($N_j = 4$ actual compared to $N_j = 4$ approximate). The close match between the two curves, however, suggests that including harmonics higher than the first four will result in only negligible changes. The figure also shows that the inclusion of higher harmonics in the blade dynamics results in differences in the actual flapping moment, as seen when the actual flapping moment for the case of including the first four harmonics in the blade motion ($N_j = 4$) is compared with the case of including only the first harmonic ($N_j = 1$).

An important and interesting result to note is that despite the difference in the actual flapping moment between the cases $N_j = 1$ and $N_j = 4$, the first harmonic approximation to the actual flapping moment for the case $N_j = 4$ is almost identical to the first harmonic approximation to the actual flapping moment for the case of $N_j = 1$. This explains why the first harmonic approximation gives such good results in flight mechanics problems where frequencies of only up to 1/rev are of interest. This fact is further illustrated in Fig 4 which depicts the total lift transferred from a blade to the hub.

In order to increase the model efficiency in trim calculations, the direct integration with respect to time is replaced by a solution of a fairly large nonlinear periodic problem. This problem is solved using a new method of obtaining numerical solutions for highly nonlinear periodic problems (Ref 18).

Thus, the present Technion Model offers a very convenient way of changing the accuracy of the rotor model. By choosing values of N_j between 1 and very large, one is capable of "moving continuously" between a "tip path plane" approach and a classical blade-element straightforward integration with respect to the azimuth.

Results

The ability of each model to correctly simulate the flight mechanics of the AH-64 was determined by comparisons with available flight test data. The comparisons were performed by trimming the simulation models to the flight condition being considered and driving the models with the recorded flight test control inputs in all axes. To prevent the trim discrepancies between the models and the actual flight vehicle from affecting the dynamic response comparisons, calculated variations from the flight-test-

control trim values were used in constructing the simulation inputs. In other words, the simulation control inputs consisted of the sum of the simulation trim values and the flight test control variations from trim. Both the on- and the off-axes responses of the models were looked at and compared with flight-test data. This paper, however, concentrates on the on-axis responses for the sake of brevity, and includes only one off-axes case for completeness. The difficulties of matching coupled responses are also briefly discussed.

Data obtained under contract from MDHC were used for the model comparison work presented here. In addition to being the best data available, the use of the MDHC data allows a comparison of the responses of the new models with the MDHC model FLYRT, since the same data were used for validating FLYRT as outlined in Ref 8. The reader is referred to that document for information regarding flight conditions, processing, and consistency checks/corrections performed by MDHC.

Even though the Technion Model and BEMAP are completely different in origin and design, they are based on the same set of wind-tunnel and flight-test data. Furthermore, they both employ the same basic modeling approaches in all the modules except the main rotor. The major differences between the two rotor-modeling approaches documented above may be summarized as follows:

1. BEMAP uses a direct blade-element approach which considers all the harmonics, whereas the Technion Model includes only the first harmonic since the first harmonic was shown to almost solely dominate the aircraft response for flight mechanics applications.
2. The Technion Model uses the Pitt/Peters (Ref 19) dynamic inflow model while BEMAP can use either Pitt/Peters or the "extended" Howlett inflow model described by Ballin (Ref 20). The two inflow models are quite similar, as confirmed by comparing BEMAP responses using Pitt/Peters with BEMAP responses obtained using the extended Howlett model.
3. The airfoil tables used for both models are the same (Ref 10). However, whereas BEMAP incorporates look-up tables for calculating section forces, the Technion Model uses polynomial fits of the data in the rotor derivations.
4. The Technion Model does not consider the lead/lag degree of freedom whereas BEMAP does. This, however, does not necessarily help BEMAP because of the unavailability of a good model of the elastomeric lead-lag dampers used on the Apache.

Static Validation

Static validation refers to the comparison of the equilibrium trim conditions of the aircraft and simulation models.

Figures 5a-f show that both models simulate the trim controls and the attitudes of the helicopter quite well across a range of airspeeds. The trim comparisons do not point to a clear choice as far as modeling the rotor is concerned since the models alternately come closer to the flight data as is seen from the figures. For example, figure 5a shows that BEMAP consistently underestimates the trim pitch attitude of the aircraft, up to a maximum error of about 2 degrees, above an airspeed of around 40 knots. Also, as figure 5b indicates, the direct blade-element model overestimates the collective input required to trim by slightly over half an inch in the range of 40 to 80 knots whereas the harmonic model does quite well up to around 120 knots. In calculating longitudinal cyclic required to trim, however, BEMAP duplicates the trends in the flight data quite accurately whereas the Technion Model is slightly off at lower speeds, as may be seen in figure 5c. The same is true for the lateral cyclic required to trim, as may be seen in figure 5e. Finally, figures 5d and 5f show that the two models are quite comparable as far as calculating the trim roll angle and trim directional control are concerned. Therefore, until further work has determined the cause of the discrepancies in each model, neither can be judged better or worse than the other.

Dynamic Validation

Dynamic validation refers to the comparison of the dynamic response characteristics of the aircraft and simulation model following a control input away from trim. Dynamic response is much more difficult to simulate accurately than trim because the random conditions present at the time of the flight tests, such as wind and turbulence, affect the responses of the aircraft but are difficult to record or model. Post processing schemes to remove the random, uncorrelated responses may be used to reduce the severity of the problem (Ref 21), but none were attempted here.

The on-axis responses of both models are good (only DASE-off data were considered for this work). Concentrating on the slopes of the various coplotted lines in Figs 6-11, rather than the absolute values, we see that in almost all the cases both models simulate the overall response fairly accurately. The mismatches usually seem to be in the form of a bias starting from a mismatch of trim conditions. Both models seem to overpredict the rate of onset of the accelerations by about the same amount. This is interesting given the fact that the rotor is mostly responsible for the accelerations and that the two models use completely different rotor modules. The secondary effects not modeled by either model, as opposed to the differences between the two models, are most likely responsible for the variations from the actual aircraft response. These secondary effects include compressibility, reverse flow, and tip losses.

It is also interesting to note that the Technion Model seems to correlate better in the lateral axis, whereas BEMAP seems to correlate better in the longitudinal, regardless

of flight condition. The lateral responses of the BEMAP model at both hover and 80 kts (Figs 6 and 7) is seen to be less damped than the Technion Model whereas the longitudinal responses of the BEMAP model (Figs 8 and 9) seem to be overall closer to the flight data than the Technion Model. One possible reason for this may be the lead-lag degree of freedom. The Technion Model does not consider the lead-lag and it appears that, at least as far as lateral response is concerned, not considering the lead-lag may be better than considering it without a representative model of the dampers.

Figures 10 and 11 depict the directional responses of the models to directional doublets at hover and 80 kts, respectively. As may be seen, in both cases BEMAP trims with excessive right pedal and fails to correlate with flight data as well as it does in the other axes. The Technion Model, on the other hand, does quite well at hover and somewhat better than BEMAP at 80 kts. Introduction of a good lead-lag damper may improve BEMAP in this axis as well.

The off-axis responses of both models are generally less accurate than the on-axis. Figure 11 shows the lateral response to a longitudinal doublet at hover. As may be seen, both models trim quite well but do not seem to duplicate the dynamic response very accurately. This is to be expected since the off-axis response is dominated by coupling and secondary effects which are difficult to model accurately.

Concluding Remarks

Both the BEMAP and the Technion Models are still in the development phase and are being continually updated to improve their accuracy and sophistication as necessary. Secondary effects such as compressibility, reverse flow, and tip loss have not yet been sufficiently incorporated in either model. As seen from the results presented, however, even at this stage both models are capable of simulating the response of the AH-64 helicopter quite closely. Currently, flight tests are being conducted at the Army Aviation Flight Activity (AEFA) to provide additional data to resolve the validation discrepancies.

References

1. Johnson, Wayne, A Comprehensive Analytical Model of Rotorcraft Aerodynamics and Dynamics. NASA TM-81183, 1980.
2. Aiken, E. W.: A Mathematical Representation of an Advanced Helicopter for Piloted Simulator Investigations of Control-System and Display Variations, NASA TM-81203, 1980.
3. Talbot, P. D., Tinning, B. E., Decker, W. A., and Chen, R. T. N., A Mathematical Model of a Single Main Rotor Helicopter for Piloted Simulation, NASA TM-84281, 1982.

4. Harrison, J. M., An Integrated Approach to Effective Analytical Support of Helicopter Design and Development. Paper presented at the Sixth European Rotorcraft and Powered Lift Aircraft Forum, Sept. 1980.
5. Howlett, J. J., UH-60A Black Hawk Engineering Simulation Program: Volume I – Mathematical Model, NASA CR-166309, 1981.
6. Ballin, M. G., Validation of a Real-Time Engineering Simulation of the UH-60A Helicopter, NASA TM-88360, 1987.
7. The Mathlab Group, MACSYMA Reference Manual, Laboratory for Computer Science, MIT, Version 10, Volumes I and II, January 1983.
8. Harding, J. W. and Bass, S. M., Validation of a Flight Simulation Model of the AH-64 Apache Attack Helicopter Against Flight Test Data. Proceedings of the 46th Annual Forum of the AHS, Vol. II, May 1990.
9. Chen, R. T. N., Flap-Lag Equations of Motion of Rigid, Articulated Rotor Blades with Three Hinge Sequences, NASA TM-100023, 1987.
10. Acker, G. F., et. al., Air Vehicle Technical Description Data for the AH-64 Advanced Attack Helicopter. Hughes Helicopter, Inc., Report No. 77-X-8002-3, March 1984.
11. Rosen, A. and Beigelman, Z., A Simplified Model of the Influence of Blade Elastic Pitch Variations on Helicopter Rotor Flapping Dynamics, Vertica, Vol. 7, 1983, pp. 335-360.
12. Rosen, A. and Beigelman, Z., Further Investigation of the Coupled Flapping and Torsion Dynamics of Helicopter Rotor Blades, Israel Journal of Technology, Vol. 21, 1983, pp. 104-116.
13. Rosen, A. and Beigelman, Z., The Influence of Different Inflow Models on the Coupled Flapping and Torsion of Helicopter Rotor Blades. Proceedings of the 8th European Rotorcraft Forum, Aug. 31-Sept. 3, 1982, Paper No. 3-10.
14. Menaker, D. and Rosen, A., A Model for Helicopter Performance Calculations, Vertica, Vol. 12, No. 1/2, 1988, pp. 155-178.
15. Beigelman, Z. and Rosen, A., A Simulation Model of a Single Rotor Helicopter. Proceedings of the 31st Israel Annual Conference on Aviation and Astronautics, Feb. 1990, pp. 27-37.
16. Peters, D. A. and Ha Quang, N., Dynamic Inflow for Practical Applications, Journal of the American Helicopter Society, Vol. 33, No. 4, 1988, pp. 64-68.
17. Rand, O. and Gessow, A., Model for Investigation of Helicopter Fuselage Influence on Rotor Flowfields, Journal of Aircraft, Vol. 26, No. 5, 1989, pp. 401-402.
18. Rand, O., Harmonic Variables—A New Approach to Nonlinear Periodic Problems, Journal of Computers and Mathematics with Applications, Vol. 15, No. 11, 1988, pp. 953-961.
19. Pitt, D. M. and Peters, D. A., Theoretical Prediction of Dynamic Inflow Derivatives, Vertica, Vol. 5, 1981, pp. 21-34.
20. Ballin, M. G., Validation of the Dynamics Response of a Blade-Element UH-60 Simulation Model in Hovering Flight. Presented at the 46th Annual Forum of the American Helicopter Society, Washington, DC, May 1990.
21. Tischler, M. B. and Cauffman, M. G., Frequency-Response Method for Rotorcraft System Identification with Applications to the BO-105 Helicopter. Presented at the 46th Annual Forum of the American Helicopter Society, Washington, DC, May 1990.

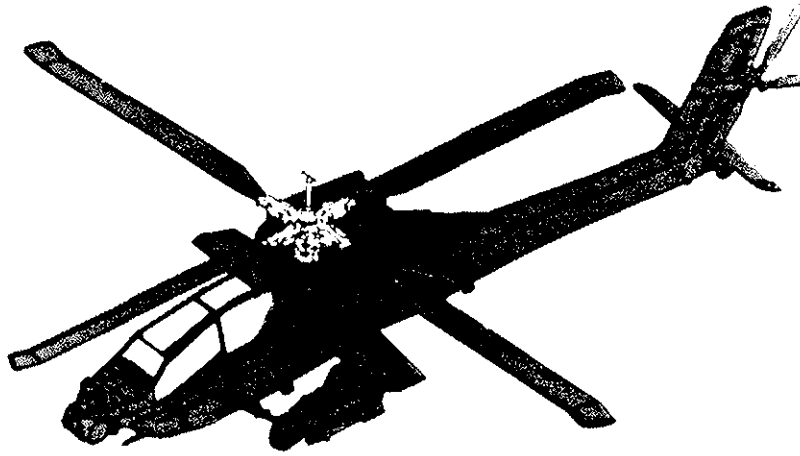


Fig 1: AH-64 Apache Advanced Attack Helicopter.

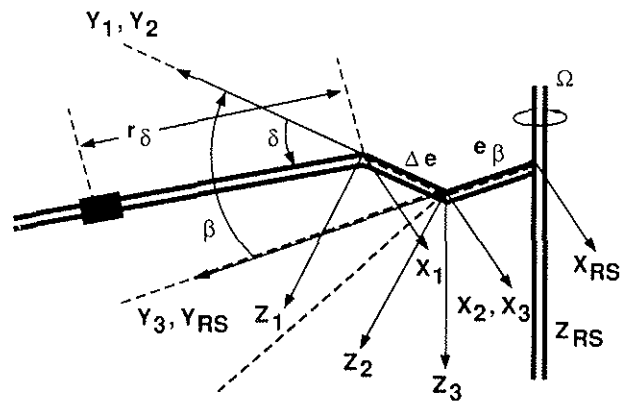


Fig 2: Coordinate system definitions for the Blade-Element Rotor derivations.

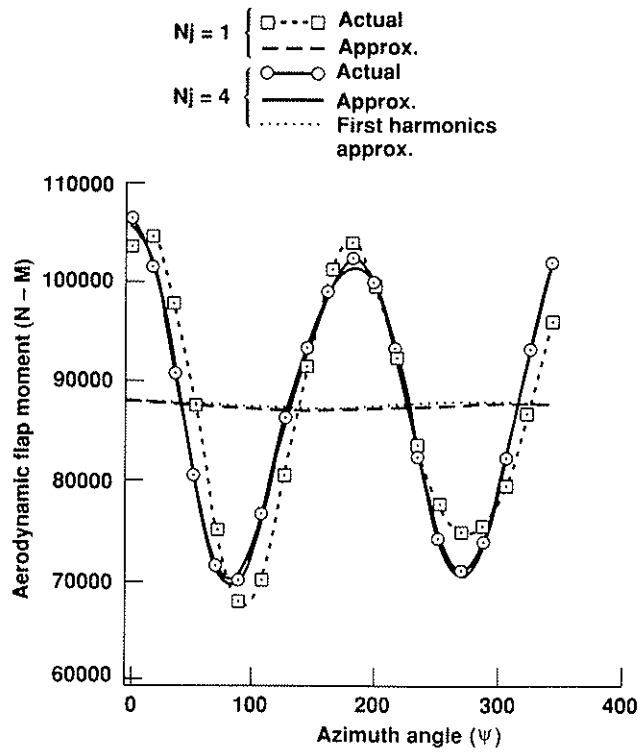


Fig 3: Aerodynamic flap moment versus azimuth angle.

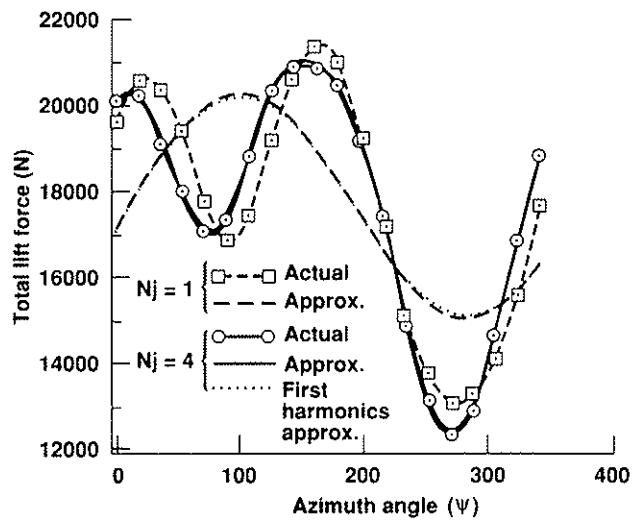


Fig 4: Total lift force versus azimuth angle.

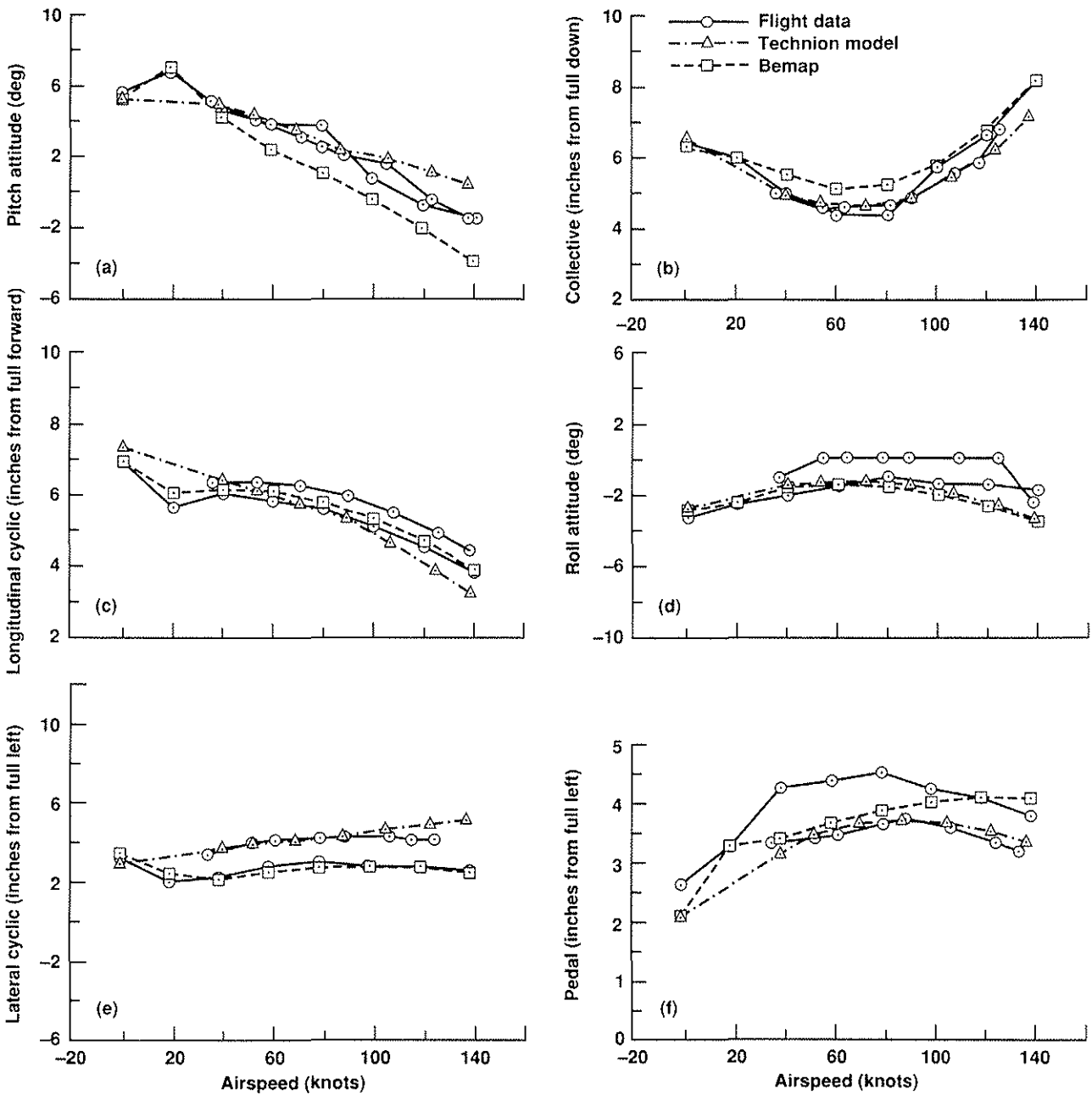


Fig 5: (a) Trim pitch attitude versus airspeed. (b) Trim collective versus airspeed. (c) Trim longitudinal cyclic versus airspeed. (d) Trim roll attitude versus airspeed. (e) Trim lateral cyclic versus airspeed. (f) Trim pedal versus airspeed.

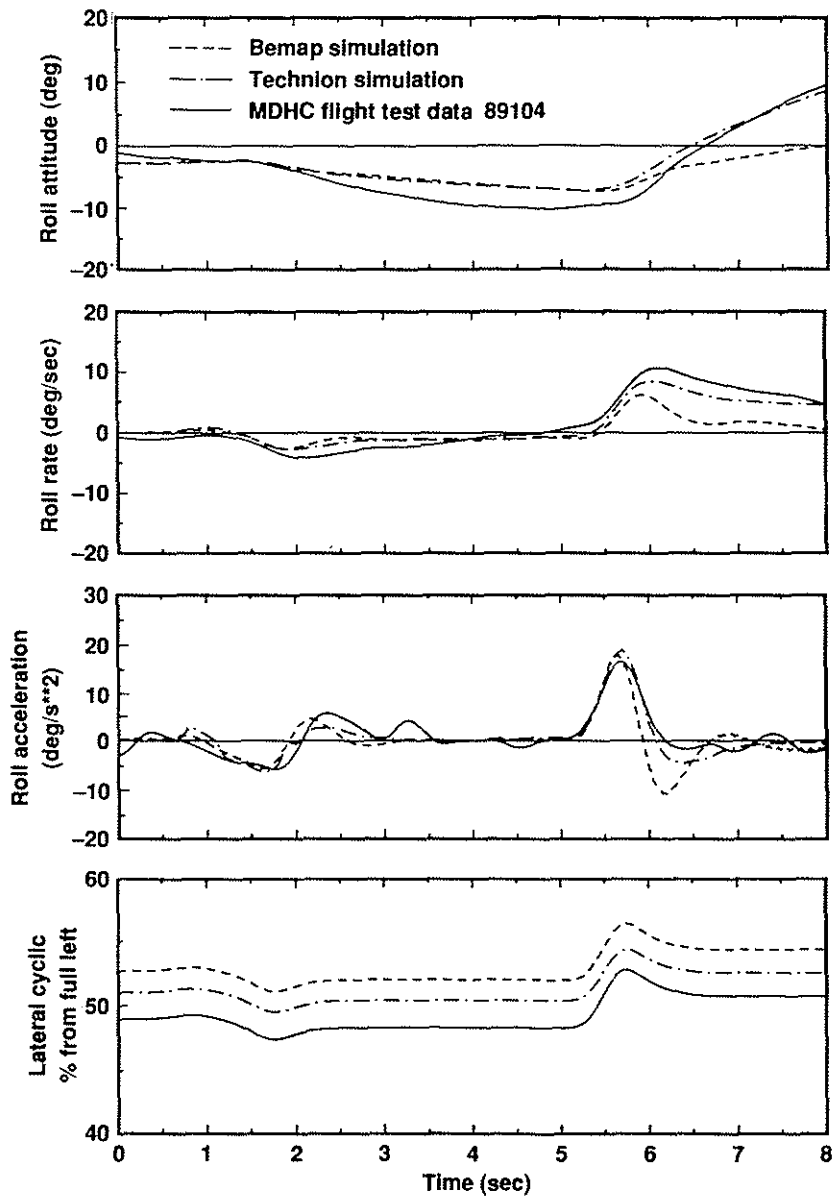


Fig 6: On-axis response to lateral doublet left, at hover.

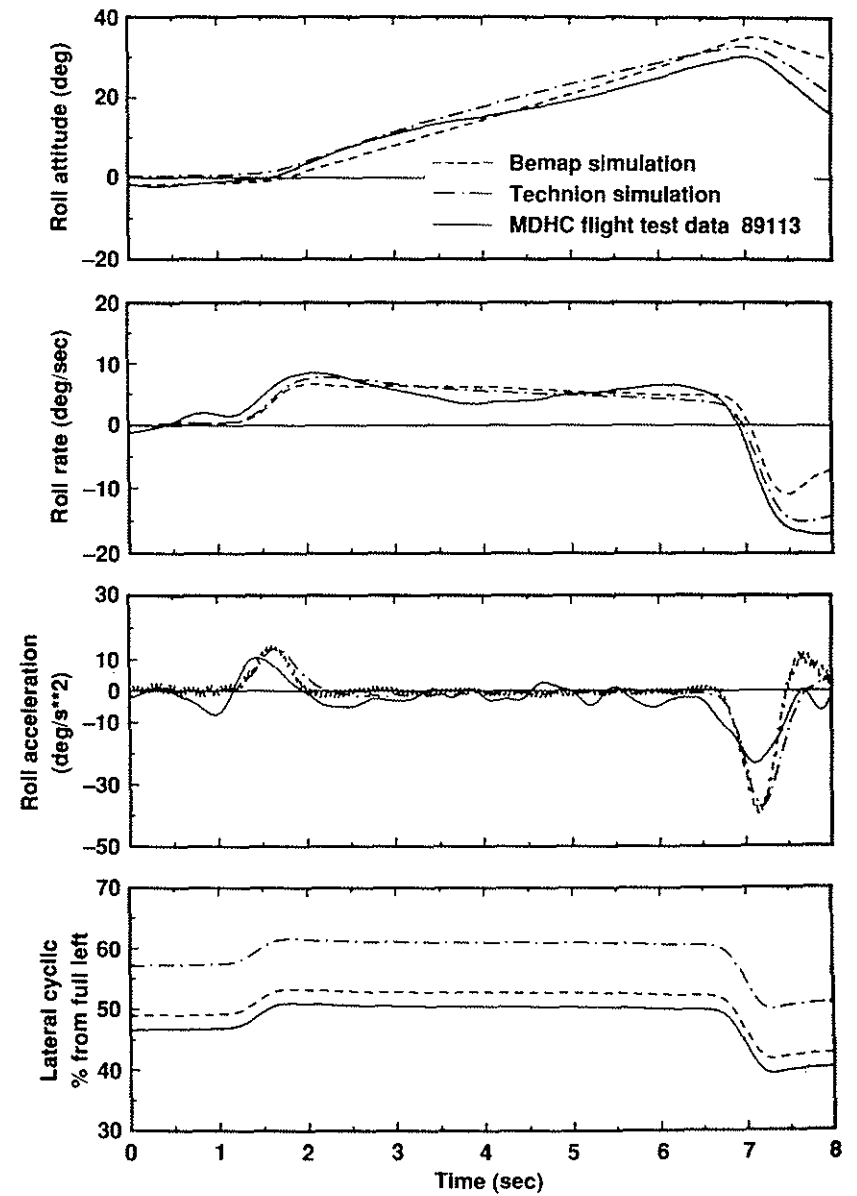


Fig 7: On-axis response to lateral doublet right, at 80 knots.

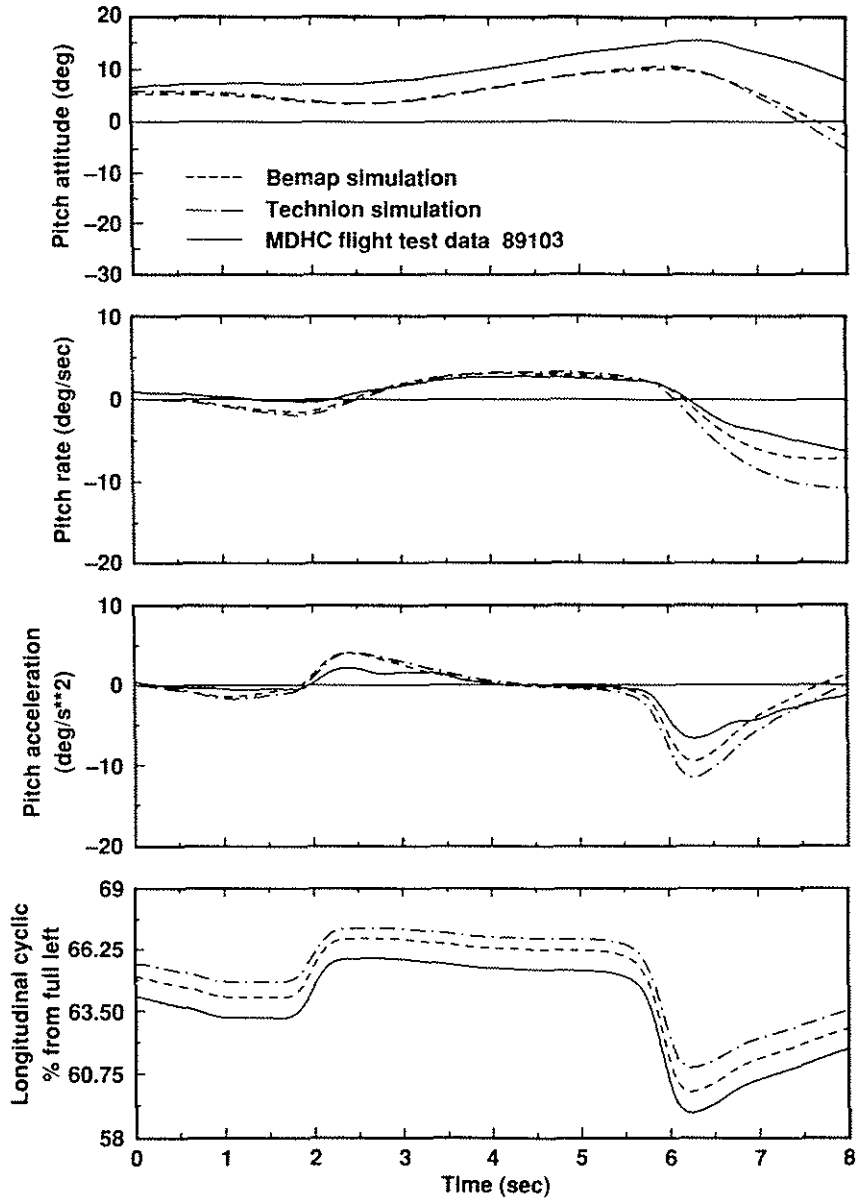


Fig 8: On-axis response to longitudinal doublet aft, at hover.

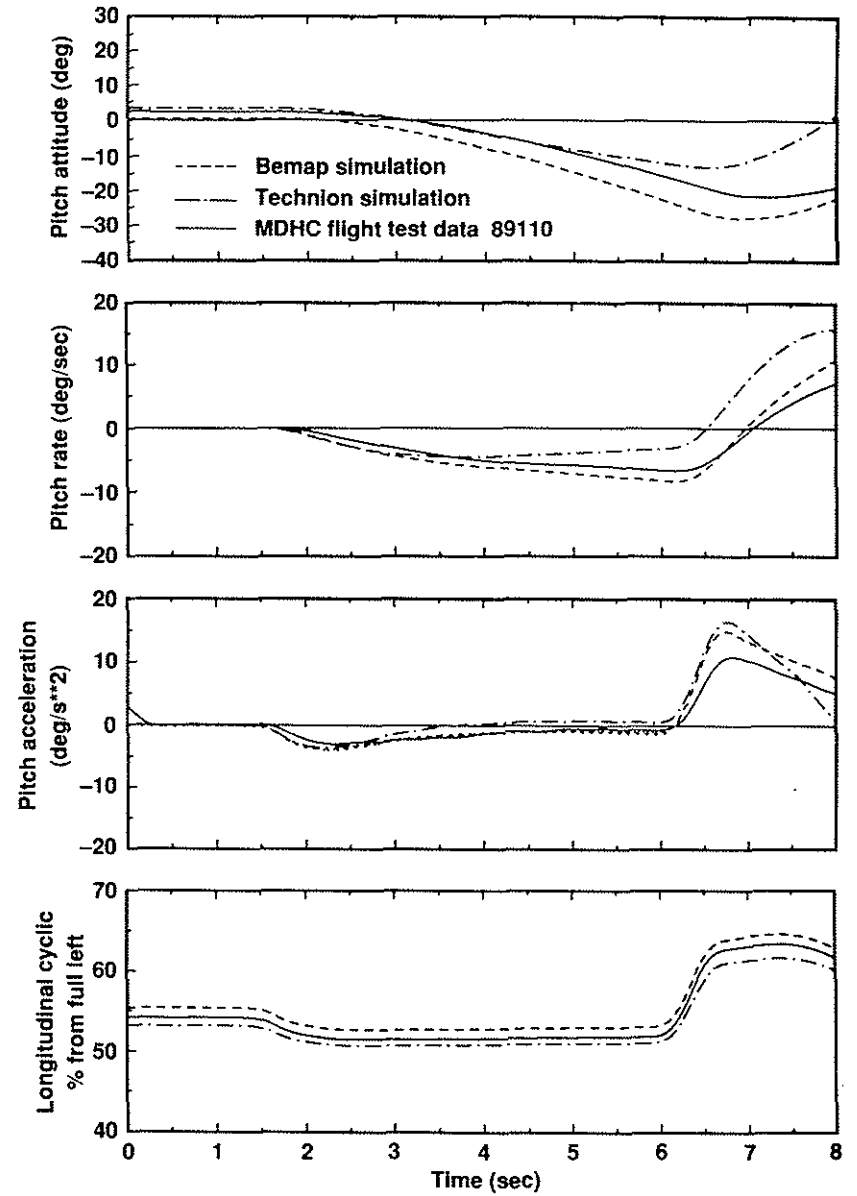


Fig 9: On-axis response to longitudinal doublet forward, at 80 knots.

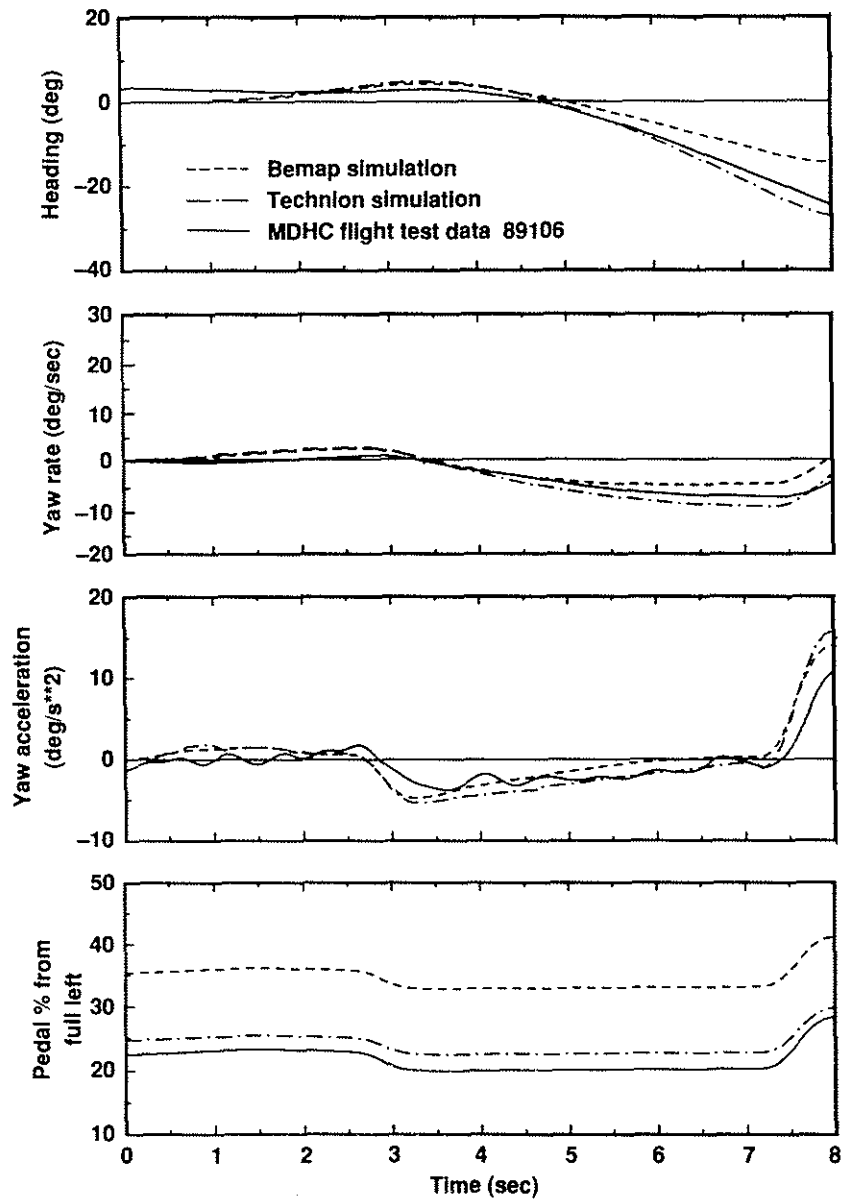


Fig 10: On-axis response to directional doublet left, at hover.

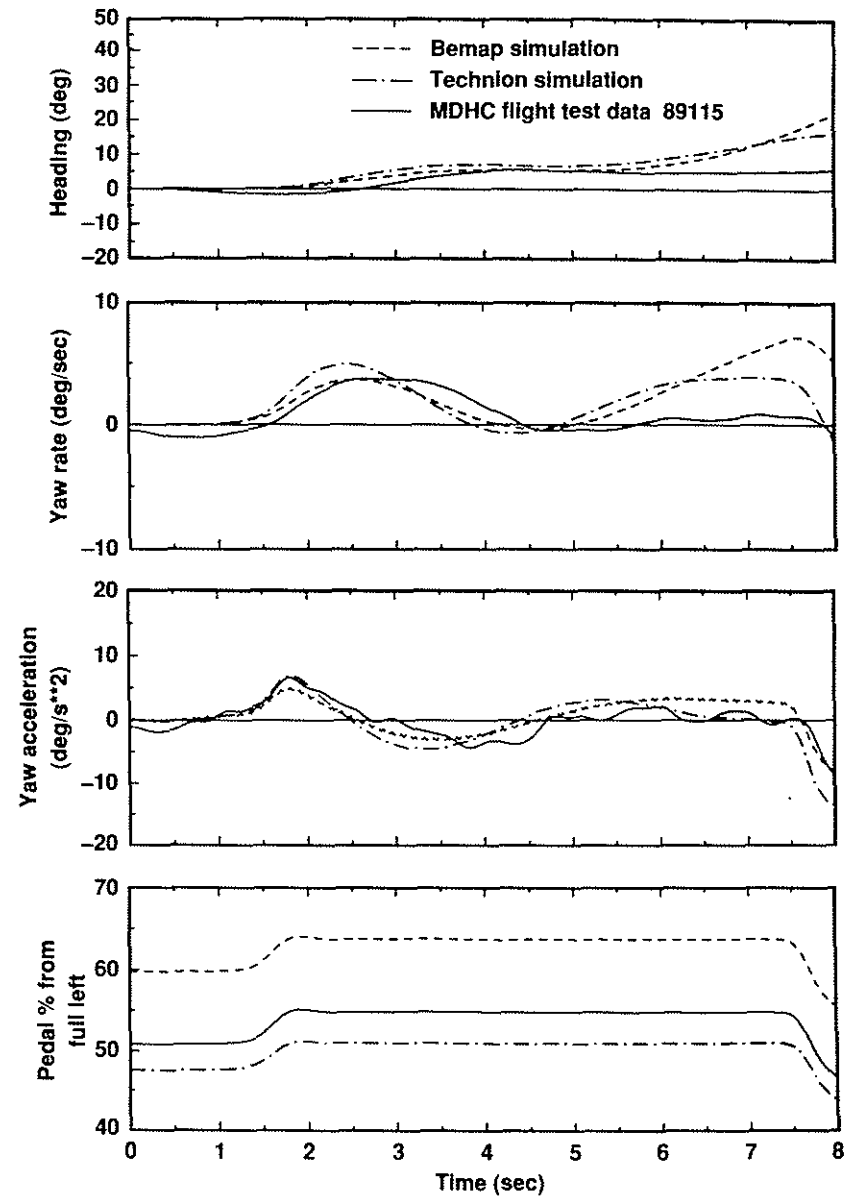


Fig 11: On-axis response to directional doublet right, at 80 knots.

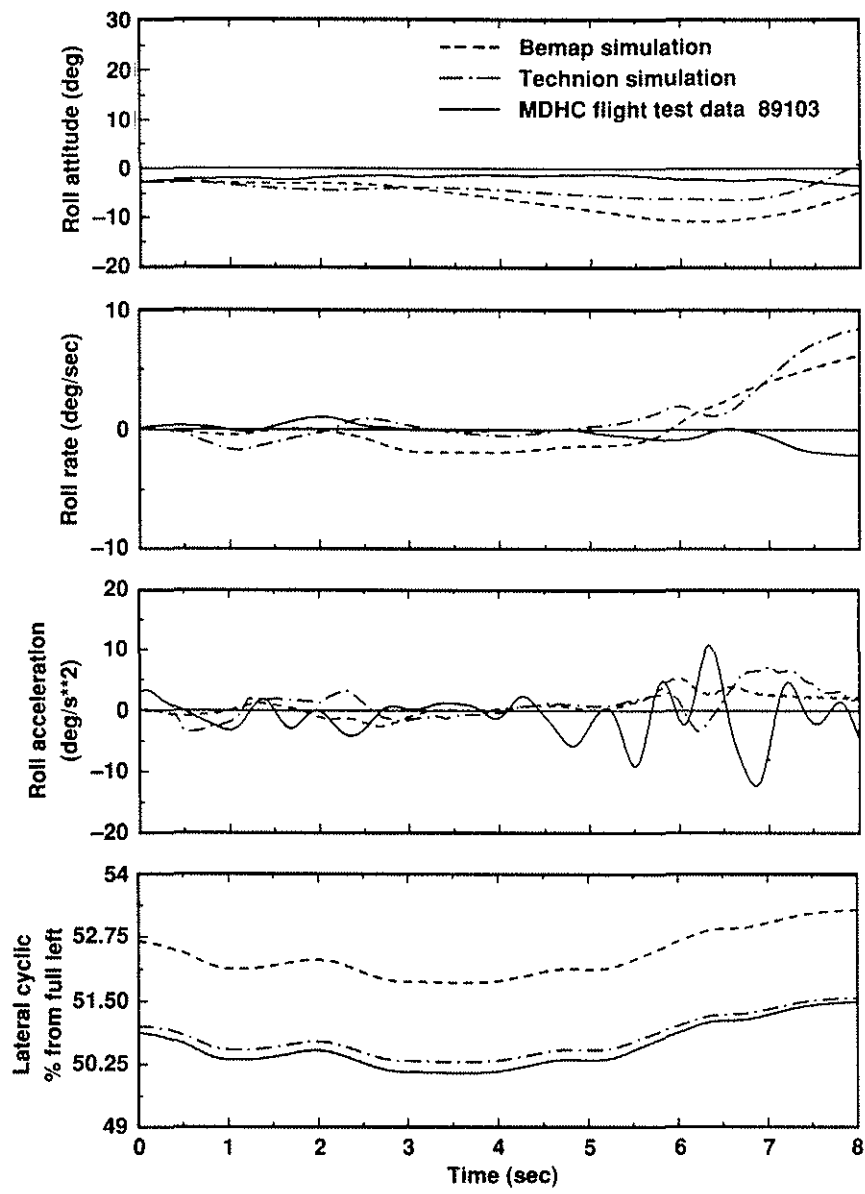


Fig 12: Lateral response to longitudinal doublet aft, at hover.